International Symposium COMODIA 90: 595-600(1990)

Comparison of 3-D Modeling of D.I. Diesel Engine Combustion with Gas Sampling Experiment

K.Nishida and H.Hiroyasu

Department of Mechanical Engineering
University of Hiroshima
Shitami, Saijo-cho
Higashi-Hiroshima 724
Japan

M.Arai

Gunma University

S.Yoshikawa

Yanmar Diesel Engine Co., Ltd.

ABSTRACT

This paper describes a total in-cylinder sampling experiment and a three-dimensional computation on combustion and emission formation processes in direct injection (D.I.) diesel engines. The sampling method consisted of rapidly opening a blowdown valve attached to the bottom of the piston cavity, and quickly transferring most of the in-cylinder contents into a large sampling chamber. The sampling experiment gave a history of the spatially-averaged composition in the cylinder. In the computation, the spray trajectory, fuel vaporization, gas motion and combustion were modeled simply based on the experimental results and empirical equations. The dispersion of the gaseous components and the enthalpy was computed by solving the conservation equations with the finite difference technique. The breakup time of the spray was varied in the computation for expressing the experimental results of the processes of the combustion and the formation of nitric oxide and soot under various length-to-diameter ratios of the nozzle hole.

INTRODUCTION

Current development work of direct injection (D.I.) diesel engines with low emissions, such as nitric oxide and soot, as well as improved fuel economy requires a better understanding of the combustion and emission formation processes in the cylinder. Both detailed experimental data and improved combustion models should help in the efforts to meet these objectives. Especially, data which gave the time- and the space-resolved histories of the in-cylinder contents were needed. Such in-cylinder data were obtained by use of a rapid sampling probe (1)-(3). Probe studies were, however, limited to sampling from the local volume in the cylinder, and were not suitable for comprehending the overall processes of the heterogeneous combustion in the D.I. diesel engine. Total in-cylinder sampling experiments, using a dumping apparatus with a rupture diaphragm installed in the cylinder head, were made to investigate the spatially-averaged composition in the cylinder(4)(5). The installation of the dumping apparatus in the cylinder head of a small-sized engine often required some modification of the intake and exhaust ports, both of which greatly influenced the combustion and emission formation. Thus, such a sampling system was not applicable to a small-sized engine.

The total in-cylinder sampling method employed in this study consisted of rapidly opening a blowdown valve attached to the bottom of the piston cavity, and quickly transferring most of the in-cylinder contents into a large sampling chamber below the piston. No modifications of the intake and exhaust ports in the cylinder head were required for the installation of this blowdown apparatus. The spatially-averaged contents of the nitric oxide, soot and total hydrocarbon were measured at a given crank angle, using various nozzles with a different length-to-diameter ratio of the nozzle hole. These influenced the breakup behaviors of the spray. A three-dimensional modeling of the mixture formation and the combustion of a D.I. diesel engine(6) was applied for the purpose of comprehending the effects of such spray characteristics on the processes of the combustion and the formation of nitric oxide and soot in the cylinder.

TOTAL IN-CYLINDER SAMPLING EXPERIMENT

Engine and Blowdown Apparatus

A four-stroke D.I. diesel engine with a bore of 78.0 mm and a stroke of 86.0 mm was used in this study. The main specifications of the engine are shown in Table 1. The engine was modified for the total in-cylinder sampling experiment as shown in Fig.1. An elongated cylinder liner with a sampling chamber and an elongated piston with a blowdown valve, a couple of cams and a rotary solenoid were installed in the engine. When the cams were rotated by the rotary solenoid at a given crank angle after the end of the injection, the cylinder pressure caused the blowdown valve to be pushed downward. Then the blowdown valve rapidly opened, and most of the in-cylinder contents quickly transferred into a large sampling chamber. This chamber had a volume of sixty times the displacement of the engine and was filled with argon quench gas. If the blowdown process was rapid and the cooling rate was high enough, the chemical reactions would thus be quenched so that the composition of the gas in the sampling chamber would be representative of the composition in the cylinder at the instant of the blowdown.

Sampling Procedure

The engine was driven by an electric motor at

Table 1 Engine specifications

Bore	78.0 mm
Stroke	86.0 mm
Swept Volume	$1.64 \times 10^3 cm^3$
Compression Ratio	16.5
Cavity Type	Cylindrical
Injection Pump	Bosch-AD
— Plunger Diameter	7.5 mm
Injection Nozzle	DL150S234
— Number of Holes	4
— Hole Diameter	0.23 mm
— Cone Angle	150.0 deg
— Opening Pressure	19.6 MPa

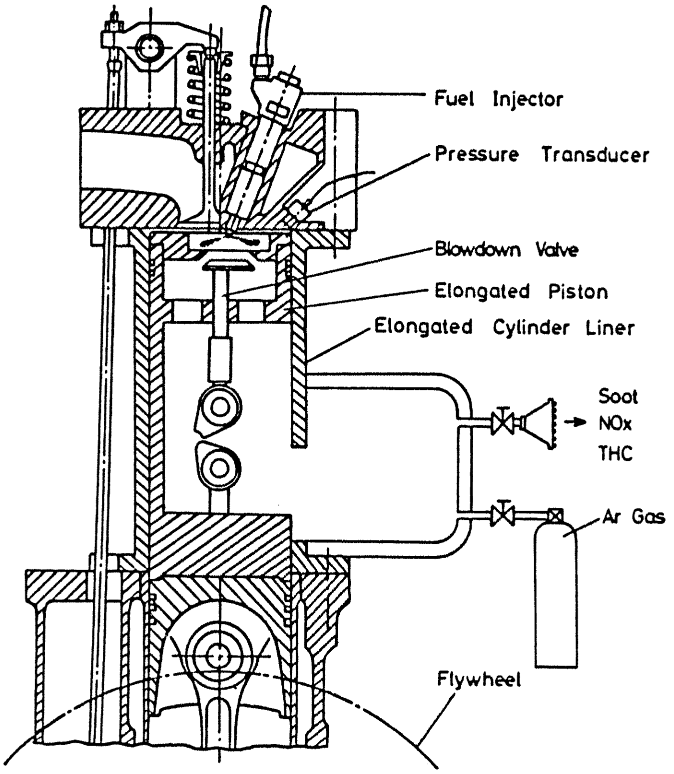

Fig.1 Modified engine for a total in-cylinder sampling experiment

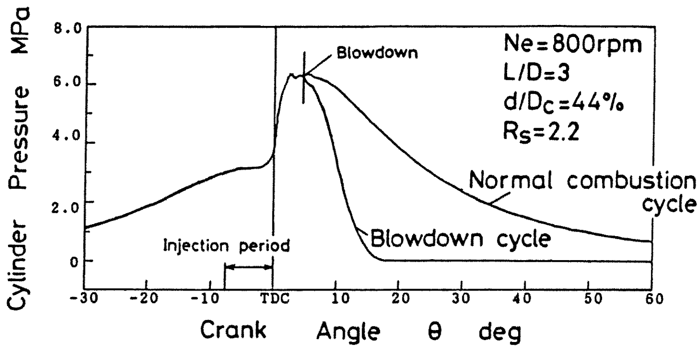

Fig.2 Typical pressure traces in blowdown and normal combution cycles

a constant speed, and then a single injection of fuel was made by actuating a control rack only in the blowdown cycle. At the beginning of the compression stroke in the blowdown cycle, the intake and exhaust valves were deactuated by pulling the spacers inserted between the push rod and the rocker arm so that the sampling chamber was isolated from the intake and exhaust ports. The intake air and cooling water in the cylinder head were heated up to 150 °C and 90 °C respectively to get an ignition delay and combustion pressure the same as those of a running engine.

All of the blowdown system, consisting of the blowdown valve actuation, the valve train isolation and the single fuel injection, was controlled by a computer. The computer was also used for the acquisition of the cylinder pressure, fuel injection pressure, needle lift signal and crank angle signal, and for the calculation of the rate of heat release in the normal combustion cycle without the blowdown. The beginning of the blowdown was determined by a comparison between the pressure traces in the blowdown and the normal combustion cycles.

The gas in the sampling chamber was sucked out by a vacuum pump through a glass fiber filter to gas analyzers. The filter samples were weighed after drying in order to determine the non-volatile mass as dry soot. The soot concentration was represented by the mass ratio of the dry soot to the amount of fuel injected. The nitric oxide and total hydrocarbon in the gas passing through the filter were measured by a chemiluminescence type NO analyzer and an FID type THC analyzer, respectively. The total hydrocarbon concentration was converted to the propane. The nitric oxide and total hydrocarbon concentrations were corrected for any argon dilution in the sampling chamber.

Evaluation of Blowdown

Figure 2 shows the typical pressure traces in the blowdown and the normal combustion cycles at an engine speed N_e=800 rpm, injection timing -8 deg. and equivalence ratio 0.8. The in-cylinder gas blew out of the combustion chamber through a blowdown port of 30.0 mm diameter which occupied a major portion of the bottom of the piston cavity of 34.3 mm diameter for d/D_c=44 % a ratio of the piston cavity diameter to the cylinder bore. The cylinder pressure decreased rapidly after the blowdown began at 4 deg., and the pressure half-decay angle for this experiment was 5 deg. Such a rapid decrease in the cylinder pressure and the dilution with argon gas seemed to result in enough quenching immediately after the blowdown valve opened. In this study, the concentrations of the contents in the gas quenched in the sampling chamber were assumed to be the concentrations of the in-cylinder contents at the beginning of the blowdown.

Experimental Conditions

As shown in Table 2, the length-to-diameter ratio of the nozzle hole (L/D), the ratio of the piston cavity diameter to the cylinder bore (d/D_c), the intake swirl ratio (R_s), and the injection timing (θ_{inj}) were chosen as the engine variables in the current experiment. In this paper, the results for various L/D with other engine variables fixed at d/D_c=44 %, R_s=2.2 and θ_{inj}=-8 deg. are

Table 2 Experimental conditions

Engine Speed	800 rpm
Mass of Injection Fuel	22 mg/stroke
Equivalence Ratio	0.8
Cooling Water	90 °C
Intake Air	Natural Aspirated Air Temperature 150 °C
Nozzle L/D	3, 4, 7
Combustion Chamber d/D_C	44, 54, 64 %
Swirl Ratio R_S	2.2, 2.8
Injection Timing θ_{inj}	-13, -8, -3 deg
Injection Duration	8 deg

reported. The engine speed and the amount of fuel injected were 800 rpm and 22 mg/stroke (equivalence ratio 0.8), respectively.

3-D MODELING

Outline of Model

The engine treated in the model(6) had a cylindrical cavity in the piston as well as a four-hole injector centered in the cylinder bore. The in-cylinder processes were computed by the model shown in Fig.3. The model consisted of four sub-models, such as diffusion, spray, combustion and air motion models. In the diffusion model, the combustion chamber was mapped with non-uniform rectangular solid cells in the cylindrical coordinates, as shown in Fig.4. The conservation equations for the fuel vapor, the combustion products and the enthalpy of the gas were set up in each computational cell. In the spray model, the spray was considered as being composed of many packages as shown in Fig.5., and the location of each package in the combustion chamber was computed. The rates of the fuel vapor generation and the heat absorption by vaporization were computed in each spray package, and were distributed to the computational cells surrounding the package as the source terms of the conservation equations. The combustion model computed the ignition delay of the mixture in the computational cell, and the irreversible, single-step chemical reaction rate of the combustible mixture after the ignition. The air motion model treated the angular swirl velocity and the radial squish velocity by a quasi-dimensional method(7). The conservation equations for the gaseous components and the enthalpy were numerically solved in the flow field with the swirl and squish by the finite difference technique. And the spatial concentration distributions of the fuel vapor, oxygen and

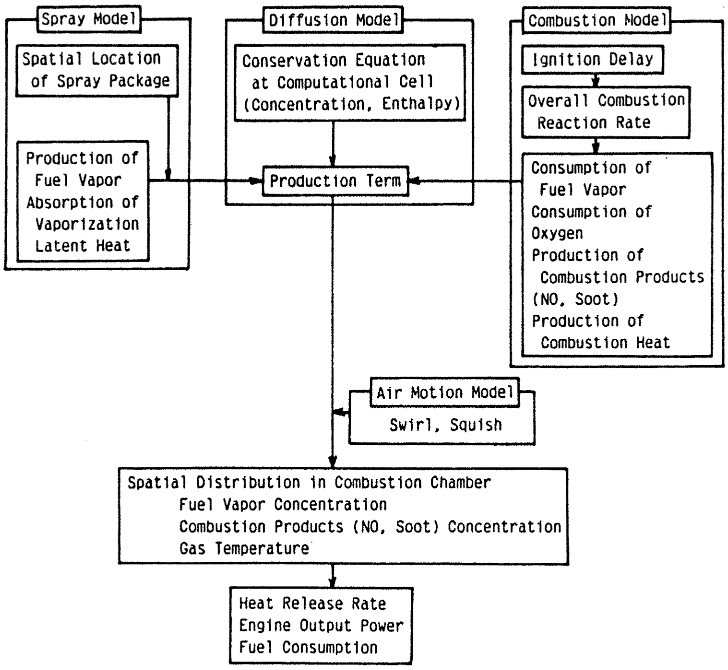

Fig.3 Flow diagram of the computational model

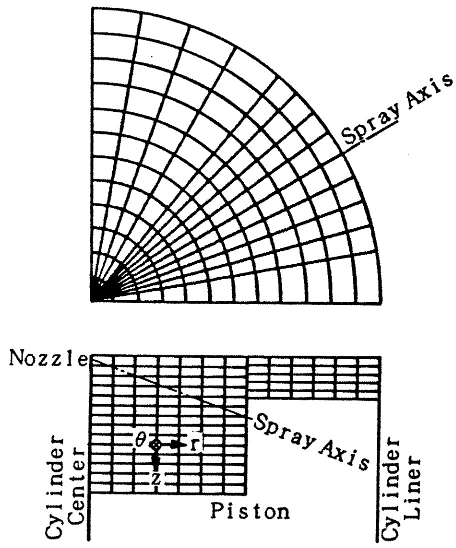

Fig.4 Computational domain and coordinates

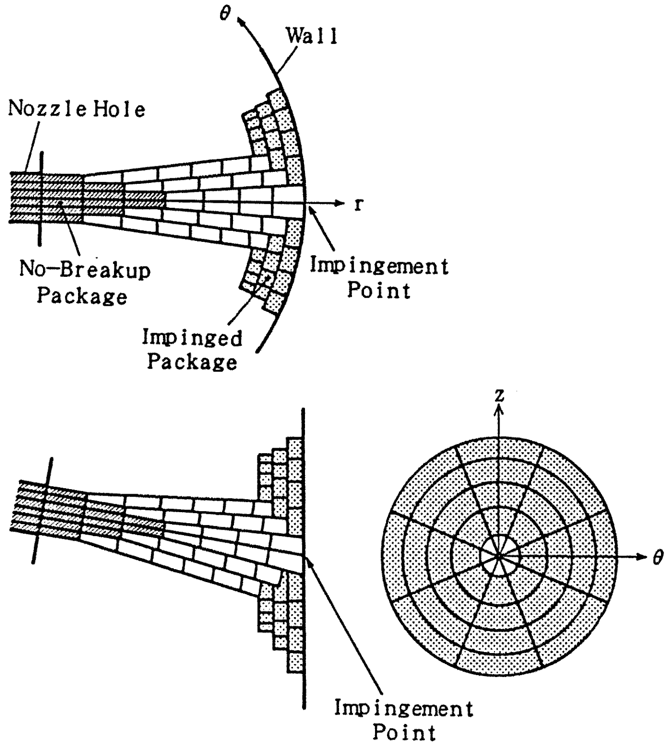

Fig.5 Penetration of spray packages in an impinging spray

combustion products (nitric oxide and soot), and the spatial gas temperature distribution were obtained at each crank angle.

Spray Model

The trajectory of each package in the spray was computed based on the empirical equations of the spray tip penetration incorporating the breakup time(8). Since the breakup time of the package at the edge of the spray was shorter than the inner packages, the radial variation of the breakup time in the spray was incorporated as follows :

$$t_b(M) = 28.65 \frac{d_0}{(\rho_a \, \Delta P)^{0.5}} \frac{4-M}{3} \qquad (1)$$

where $t_b(M)$: breakup time of M-package
d_0 : diameter of the nozzle hole
ΔP : differential pressure of the nozzle between fuel injection and ambient gas
ρ_a : density of ambient gas

The package at the edge of the spray (M=3) began to breakup at one-third the breakup time of the package at the center of the spray (M=1). After impingement on the piston cavity wall, the package was assumed to penetrate radially from the impingement point along the wall as shown in Fig.5. As shown in Fig.6, the package penetrated at a constant velocity V_0 for the breakup time $t_b(M)$, and then the velocity decreased in proportion to $t^{-0.5}$. The penetrating velocity of the package after the impingement decreased in proportion to $t^{-0.75}$. The effect of the swirl of the ambient gas on the velocity of the package was assumed to be negligible before impingement on the wall, but was incorporated after the impingement(9).

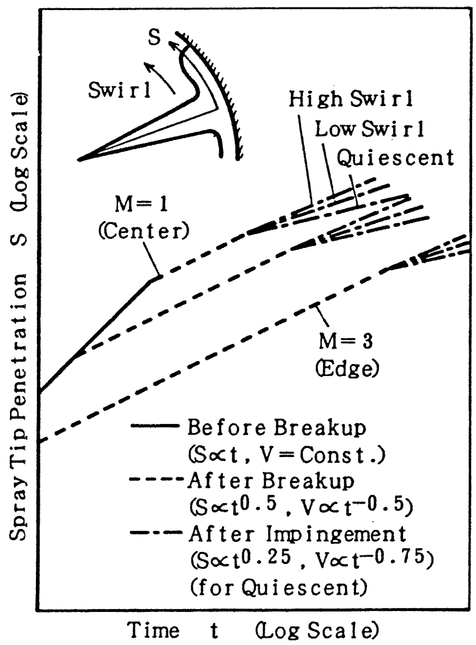

Fig 6 Tip penetration of an impinging spray

Pollutant Emissions

Eleven chemical species such as CO, CO_2, O_2, H_2, H_2O, OH, H, O, N_2 and NO were taken into consideration for predicting the pollutant emissions in the computational cell. Nine species except for the N and NO were assumed to be equal to the equilibrium concentration. The NO formation was assumed to be a non-equilibrium process controlled by the extended Zeldovich's mechanism. The first order reaction from the fuel vapor was assumed to be the soot formation mechanism, and the second order reaction between the soot and the oxygen was assumed to be the soot oxidation. Therefore the following equations were introduced in the present computations :

$$\frac{dm_s}{dt} = \frac{dm_{sf}}{dt} - \frac{dm_{sc}}{dt} \qquad (2)$$

$$\frac{dm_{sf}}{dt} = A_f \, m_{fg} \, P^{0.5} \exp\left(-\frac{E_{sf}}{R\,T}\right) \qquad (3)$$

$$\frac{dm_{sc}}{dt} = A_c \, m_s \frac{P_{O2}}{P} P^{1.8} \exp\left(-\frac{E_{sc}}{R\,T}\right) \qquad (4)$$

where m_{sf} : mass of formed soot
m_{sc} : mass of oxidized soot
m_{fg} : mass of fuel vapor
m_s : mass of soot.

E_{sf} and E_{sc} were assumed to be 1.25×10^4 kcal/kmol and 1.4×10^4 kcal/kmol, respectively(10). A_f and A_c were the constants which were determined so as to match the computed soot with the experimental results.

RESULTS AND DISCUSSION

Experiment

Figures 7 (1) and (2) show the spatially-averaged concentrations of the nitric oxide (NOx), soot (Particulate) and total hydrocarbon (THC) for L/D=3 and 7, respectively, obtained from the sampling data. The two upper curves in the figure show the cylinder pressure and the rate of heat release (R.O.H.R) in the normal combustion cycle. The histories of the in-cylinder composition for L/D=3 could be read from Fig.7 (1) as follows : Both nitric oxide and soot formed rapidly, reaching peak values by a late stage of the diffusion burning period. The nitric oxide showed an almost constant value until the end of the combustion cycle, whereas the soot showed a slight decrease due to oxidation. The total hydrocarbon showed a sudden decrease during the premixed burning period, and then showed a slight increase. After having a peak by the end of the diffusion burning period, the total hydrocarbon decreased gradually. As shown in Fig.7 (2), changing L/D only from 3 to 7 resulted in a decrease in the nitric oxide and a large increase in the soot during the whole combustion period. Slight decreases in maximums of the rate of heat release and the cylinder pressure could be seen as compared with the histories of the in-cylinder composition for L/D=3. The total hydrocarbon for L/D=7 showed a great increase after a sudden decrease during the premixed burning period, and had a maximum at an early stage of the diffusion burning period. Then the total hydrocarbon showed a large decrease again until the end of the combustion. The L/D of the nozzle hole influenced spray characteristics such as breakup length and tip penetration(11). The L/D also influenced the flame motion, especially after the spray impinged on the piston cavity wall in a small D.I. diesel engine(12). Differences in the histories of the in-cylinder composition seemed due to the changes of the spray characteristics and the flame motion along the piston cavity wall in the engine.

Computation

Computation was made for the different breakup

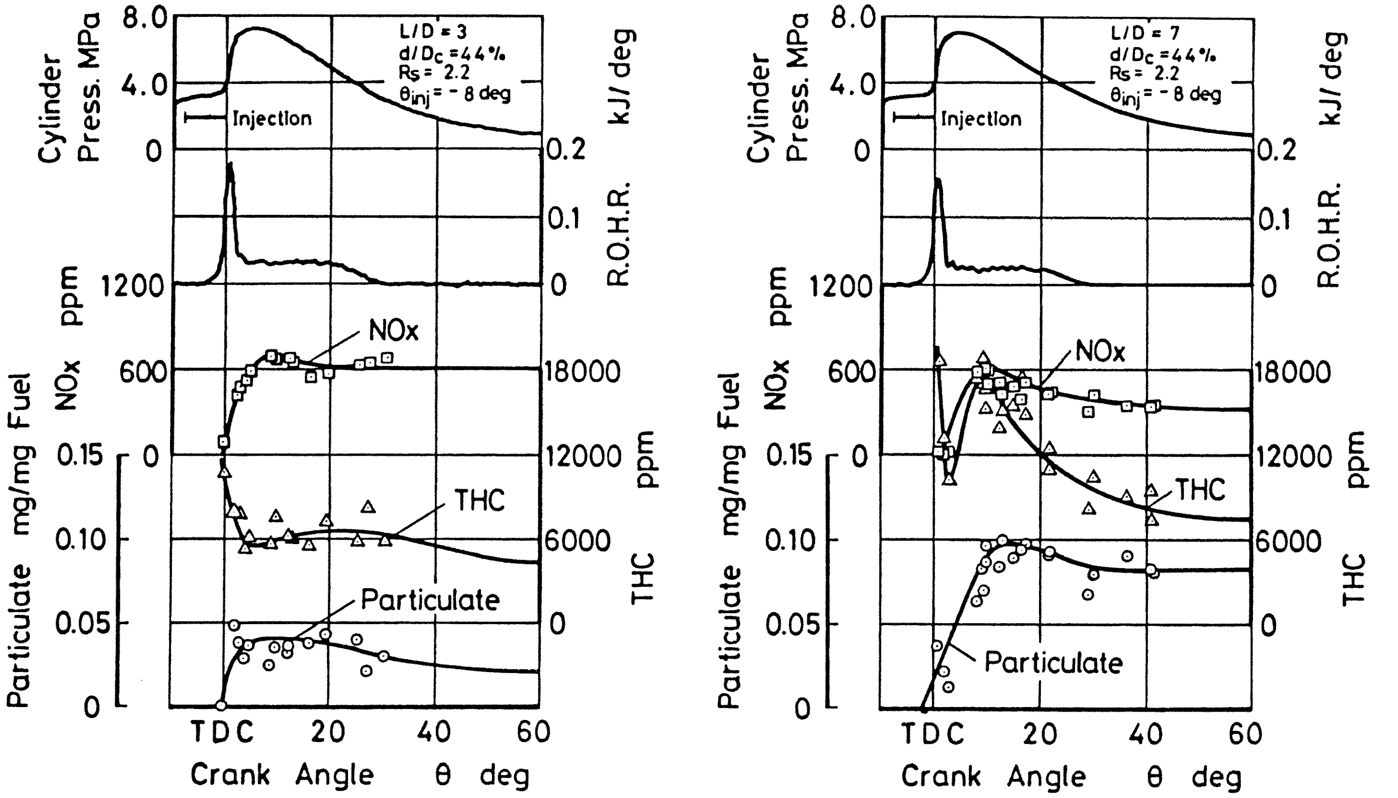

(1) L/D=3 Fig.7 Measured results of in-cylinder composition, cylinder pressure and rate of heat release (2) L/D=7

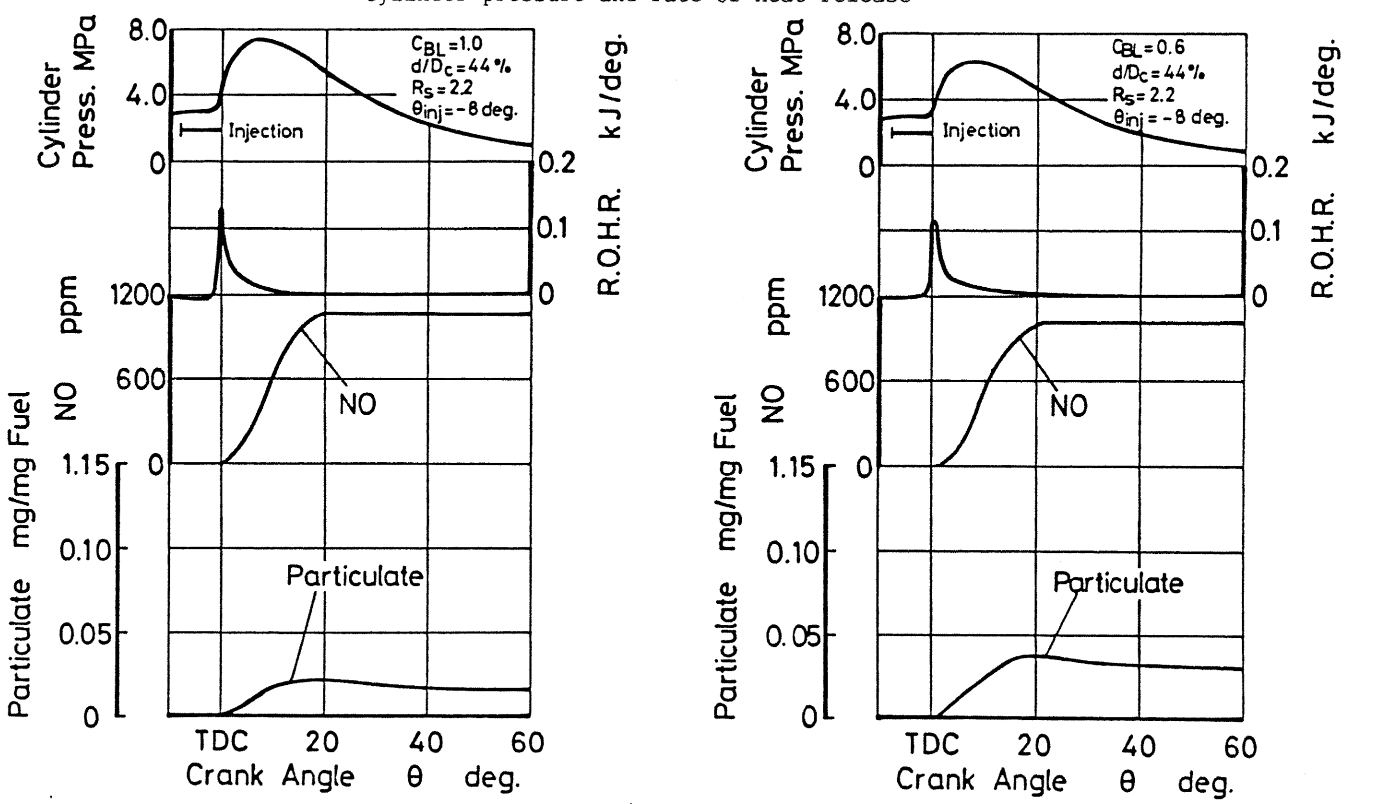

(1) Larger breakup time (C_{BL}=1.0) Fig.8 Computed results of in-cylinder composition, cylinder pressure and rate of heat release (2) Smaller breakup time (C_{BL}=0.6)

times of the spray package calculated from Eq.(1). The computed spatially-averaged concentrations of the nitric oxide, soot and total hydrocarbon, the cylinder pressure and the rate of heat release are shown in Fig.8. Figures 8 (1) and (2) are the results for the original breakup time without modification (C_{BL}=1.0), and for the breakup time shortened to three-fifths of the original value (C_{BL}=0.6). The effects of the breakup time on the spray trajectory and the fuel vapor distribution at a crank angle of the ignition are shown in Fig.9. The circles in the figure of the spray trajectory represented the locations of the injected spray packages. The fuel vapor distribution was drawn by

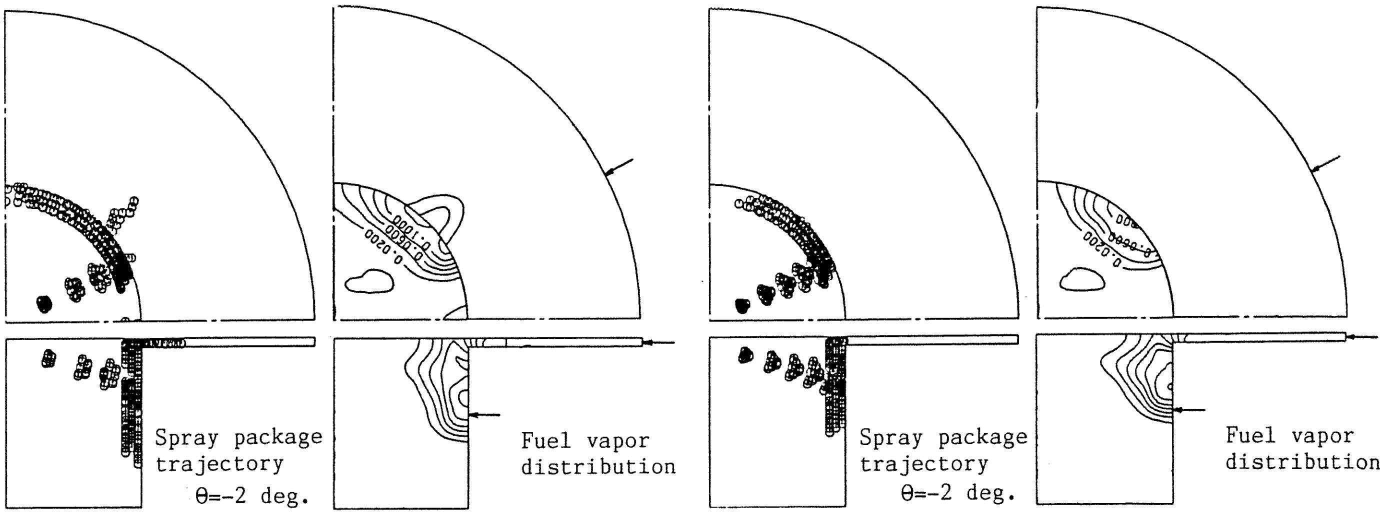

(1) Larger breakup time (C_{BL}=1.0)   (2) Smaller breakup time (C_{BL}=0.6)

Fig.9 Computed in-cylinder behaviors at ignition timing

contour lines of a mass fraction of the fuel vapor. The arrows in the contour maps represent the locations of cross sections in horizontal and vertical planes. A larger breakup time (Fig.9 (1)) resulted in a larger penetration of the spray package after, as well as before the impingement on the piston cavity wall and a wider fuel vapor distribution rather than a shorter breakup time (Fig.9 (2)). As shown in Fig.8, a larger breakup time (Fig.8 (1)) resulted in a higher nitric oxide concentration, lower soot concentration, and larger maximums of the cylinder pressure and the rate of heat release than shorter breakup times (Fig.8 (2)). These computed in-cylinder processes for larger breakup times and shorter breakup times resembled the measured results for L/D=3 and 7, respectively. Thus, the computed and measured information of the in-cylinder process implied that the variations of the breakup times of the spray due to changes of the L/D were some of the factors which dominated the combustion and emission formation processes in the D.I. diesel engine.

SUMMARY

A total in-cylinder sampling experiment and a three-dimensional computation were made for investigating the emission formation processes, such as nitric oxide and soot, in D.I. diesel engines. In the experiment, the sampling method consisted of rapidly opening a blowdown valve attached to the bottom of the piston cavity, and quickly transferring most of the in-cylinder contents into a large sampling chamber. The sampling experiment gave the history of the spatially-averaged composition in the cylinder. In the computation, the spray trajectory, fuel vaporization, gas motion and combustion were modeled simply based on the experimental results and empirical equations. The dispersion of the gaseous components and the enthalpy was computed by solving the conservation equations with the finite difference technique. The computed and measured information of the in-cylinder process implied that a variation of the breakup time of the spray, due to the length-to-diameter ratio of the nozzle hole L/D, was one of the factors which dominated the combustion and emission formation processes in the D.I. diesel engine.

REFERENCES

1. Rhee, T. K., Mayers, P. S. and Uyehara, O. A., "Time- and Space- Resolved Species Determination in Diesel Combustion Using Continuous Flow Gas Sampling," SAE Paper, No. 780226, pp. 1-28, 1978.
2. Duggal, V. K., Priede, T. and Khan, I. M., "A Study of Pollutant Formation within the Combustion Space of a Diesel Engine," SAE Paper, No. 780227, pp. 1-14, 1978.
3. Aoyagi, Y, Kamimoto, T. Matsui, Y. and Matsuoka, S., "A Gas Sampling Study on the Formation Processes of Soot and NO in a DI Diesel Engine," SAE Paper, No.800254, pp. 1-15, 1980.
4. Voiculescu, I. A. and Borman, G. L., "An Experimental Study of Diesel Engine Cylinder - Averaged NOx Histories," SAE Paper, No.780228, pp. 1-14, 1978.
5. Hedding, G. H., Kittelson, D. B., Scherrer, X. L. and Dolan, D. F., "Total Cylinder Sampling from a Diesel Engine," SAE Paper, No.810257, 1981.
6. Nishida, K. and Hiroyasu, H., "Simplified Three-Dimensional Modeling of Mixture Formation and Combustion in a D.I. Diesel Engine," SAE Paper, No.890269, pp. 53-70, 1989.
7. Murakami, A., Arai, M. and Hiroyasu, H., "Swirl Measurements and Modeling in Direct Injection Diesel Engines," SAE Paper, No.880385, pp. 1-20, 1988.
8. Arai, M., Tabata, M., Hiroyasu, H. and Shimizu, M., "Disintegrating Process and Spray Characterization of Fuel Jet Injected by a Diesel Nozzle," SAE Paper, No.840275, pp. 1-14, 1984.
9. Hiroyasu, H. and Nishida, K., "Fuel Spray Trajectory and Dispersion in a D.I. Diesel Combustion Chamber," SAE Paper, No.890462, pp. 71-88, 1989.
10. Khan, I. M., Wang, D. H. T. and Langridge, B. E., " Coagulation and Combution of Soot Particles in Diesel Engines," Comb. and Flame, 17, pp. 17-27, 1971.
11. Yoshikawa, S., Furusawa, R., Arai, M. and Hiroyasu, H., "Optimizing Spray Behavior to Improve Performance and to Reduce Exhaust Emissions in a Small D.I. Diesel Engine," SAE Paper, No.890463, pp. 89-95, 1989.
12. Yoshikawa, S., Suga, N., Nishida, K., Arai, M. and Hiroyasu, H., " An Analysis of Diesel Flame Motion by Combustion Photographs," Trans. Jpn. Soc. Mech. Eng. (Series B), 56-524, 1990.